Computational studies of influenza hemagglutinin

Boonstra, Sander

3

CHARMM TIP3P water model suppresses peptide folding by solvating the unfolded state

Abstract

The accuracy of molecular dynamics simulations depends on the underlying force field, defined by the form and parametrization of the interparticle potential functions and the water model. The treatment of the solvent is crucial in molecular dynamics force fields, as hydrophobic interactions and hydrogen bonding are important molecular forces. The widely used CHARMM force field was originally parametrized using a modified version of the TIP3P water model (mTIP3P), including Lennard-Jones interactions between hydrogens and oxygens. The latest version, CHARMM36, was optimized using the standard TIP3P water model (sTIP3P) for proteins, while mTIP3P is still being used for lipids. Our replica exchange molecular dynamics simulations on dynamic peptides show that the CHARMM36 force field with mTIP3P water yields less realistic folding than with sTIP3P water. Analysis of the dimensions and hydrogen bonding of the unfolded state reveals that the peptides are more solvated and extended in mTIP3P, due to a higher solvation energy of the peptide in this water model. We recommend using CHARMM36 with sTIP3P when simulating peptides, folded proteins, and natively unfolded proteins, but combinations of proteins with lipids would require a reparametrization to make their water models compatible.

Reprinted with permission from Boonstra S, Onck PR, van der Giessen E. 2016. CHARMM TIP3P water model suppresses peptide folding by solvating the unfolded state. *J. Phys. Chem. B* 120:3692–3698. Copyright 2016 American Chemical Society. DOI: 10.1021/acs.jpcb.6b01316

3.1 Introduction

Molecular dynamics force fields are widely used in simulations of biomolecular systems. Modern force fields have been shown to accurately reproduce properties of small peptides[3,12] and folded proteins.[22] However, the unfolded state has been shown to be much more collapsed than found in experiments, indicating that the propensity to structure formation is overestimated.[32] Force field potentials have recently been modified to better represent the equilibrium between folded and extended conformations[5,10,17] by counteracting a bias toward helical conformations.[4] This helix–coil equilibrium is determined by the balance between the intramolecular energy of a helical state and the solvation energy of more extended states.[1] For the accurate hydration of hydrophobic groups, the interplay between the protein force field and the water model plays a central role.[6]

CHARMM36,[10] the latest version of the CHARMM potential set for proteins, is the product of a recent reparametrization aimed at improving the balance between the sampling of helical and extended conformations. It was optimized using the standard TIP3P water model (sTIP3P),[19] whereas previous versions of CHARMM used a modified version of TIP3P (mTIP3P).[23] This modified version includes Lennard-Jones potentials on the hydrogen atoms of water, making them interact with both the solute and the solvent.[30] These interactions are absent in sTIP3P.

Studies with the Amber force field have shown that the use of an alternative water model can significantly influence the helix–coil equilibrium.[6,31] Since the CHARMM parameters for lipids[20] have been obtained using mTIP3P water, simulations that include a combination of proteins or peptides with lipids will have to be performed in mTIP3P water. However, this could lead to a shift in the helix–coil equilibrium, which was balanced using sTIP3P water. To explore this, we studied the influence of both water models on the helix–coil equilibrium in peptides as predicted by CHARMM36. The results of our study can have implications for all studies on peptides, proteins, and lipid systems using the CHARMM36 force field with one of the two TIP3P water models.

3.2 Method

Replica exchange molecular dynamics (REMD) simulations were used to sample the conformational space of the 3K(I)[26] and AQ[35] α-helical peptides and of the GB1[29] β-hairpin. AQ and GB1 have been used in the parametrization and validation of the CHARMM36 force field, while 3K(I) was selected to have an independent reference. In the remainder of the text, "folded fraction" is used interchangeably with helical fraction, depending on the peptide. All simulations were carried out using GROMACS 4.6.[16]

3.2.1 Water models

The water models used in this study are the standard TIP3P as published by Jorgensen et al. (sTIP3P)[19] and a modification of TIP3P (mTIP3P) that was employed during the parametrization of an earlier version of the CHARMM force field.[23] To avoid singularities in the computation of the integral equations, mTIP3P introduced Lennard-Jones interactions on the hydrogen atoms (HT) of water molecules by setting $\sigma_{HT} = 0.04$ nm and $\varepsilon_{HT} = 0.1925$ kJ/mol, instead of $\sigma_{HT} = 0$ nm and $\varepsilon_{HT} = 0$ kJ/mol as used in sTIP3P.[30] The other force field parameters, including those of the water oxygen atoms, are identical in both water models.

3.2.2 System setup and equilibration

The 3K(I) (Ace-$(AAAAK)_3$A-NH_2), AQ (Ace-$(AAQAA)_3$-NH_2), and GB1 (GEWTYDDATKTFTVTE) peptides were prepared in an extended conformation. The topologies were created using the GROMACS tool pdb2gmx and included the CHARMM CMAP correction. In agreement with the experiments, the N- and C-termini of 3K(I) and AQ were acetylated and amidated, and those of GB1 were charged. Ionizable residues were protonated according to pH 7. After a steepest descent energy minimization, the peptides were solvated in a truncated octahedral box with 2379, 2393, and 1834 molecules, respectively, of either sTIP3P or mTIP3P water. If needed, chloride or sodium atoms were added to neutralize the system. The simulation box was then energy minimized again using the steepest descent algorithm, followed by an equilibration run of 200 ps at 200 K using the Langevin thermostat, with position restraints on the peptide to relax the solvent. The temperature was set to 300 K with a 100 ps run in the NVT ensemble, after which an NPT simulation of 200 ps set the pressure to 1 bar using Berendsen pressure coupling. The resulting simulation box was scaled to the average volume of the last 50 ps.

3.2.3 Replica exchange molecular dynamics

REMD enhances sampling by exploiting the fact that energy barriers can be overcome more easily at higher temperatures and provides an ensemble average as a function of temperature. REMD simulations were run using 32 replicas in the NVT ensemble with temperatures ranging from 275 K to 427 K and replica exchange attempts every 1 ps. An NVT run of 100 ps was used to equilibrate each replica at the desired temperature. This resulted in exchange probabilities ranging from 0.25 to 0.4. Langevin integration was used with a friction coefficient of 0.2 ps^{-1}. The Langevin thermostat slightly influences the dynamics but does not affect the averages taken in equilibrium conditions.[2] A time step of 2 fs has been used while constraining all bonds including hydrogen atoms with P-LINCS[15] and keeping the waters rigid using SETTLE.[28] Long-range electrostatics was calculated using PME with a grid spacing of 1.2 Å and a direct space cut-off of 9 Å. The van der Waals

interactions were cut off at 14 Å. This runs faster than standard CHARMM settings, i.e., a switching function between 10 and 12 Å, but yields similar results. The REMD run times ranged from 500 ns to 1.1 μs, depending on the peptide and the water model.

3.2.4 Definition of folded states

Coordinates were stored every 1 ps for analysis of the peptide structure, solvation, and hydrogen bonding. A residue is regarded to be in a helical conformation if its backbone dihedral angles $\phi \in [-100^\circ, -30^\circ]$ and $\psi \in [-67^\circ, -7^\circ]$.[13] The helical fraction of a conformation is defined as the number of consecutive residues (at least three) in a helical conformation divided by the number of residues in the peptide. For 3K(I) and AQ, a conformation with zero helical fraction is called unfolded. A conformation of the GB1 peptide is regarded as being folded if the d_{RMS} with respect to all native contacts in the PDB structure (PDB: 1GB1) is smaller than 1.5 Å.[7] Native contacts lie between backbone atoms (CA, C, O, and N) with a maximum distance of 4.5 Å, but only for residues separated by at least two other residues in the sequence. The melting curves show the average helical or folded fraction over all conformations, with the error calculated as the sum of the inter- and intrablock standard error of the mean using five blocks. The cut-offs for identifying hydrogen bonds were a 3.5 Å distance and a 30° angle.

3.2.5 Convergence

All the performed simulations have converged to the equilibrium ensemble as monitored by the evolution of the helical or folded fraction. Figure 3.1 illustrates this for the case of the helical content of AQ at 275 K (similar convergence was obtained for 3K(I) and GB1). The replicas at higher temperatures generally equilibrate faster and were analyzed from the starting point of the lowest temperature replica. The unbiased converged averages for all temperatures were gathered to produce a melting curve for each of the simulated systems.

3.3 Results

3.3.1 Melting curves

The temperature dependence of the folded and helical fractions resulting from the simulations are shown in Figure 3.2, together with experimental values from the literature. Both the folded and helical fractions from the simulations using sTIP3P are consistently higher than those from the simulations using mTIP3P. CHARMM36 was parametrized to yield agreement with the experimental helical fraction of AQ at 300 K,[10] so absolute comparison between the water models should be made at this temperature. In doing so, sTIP3P

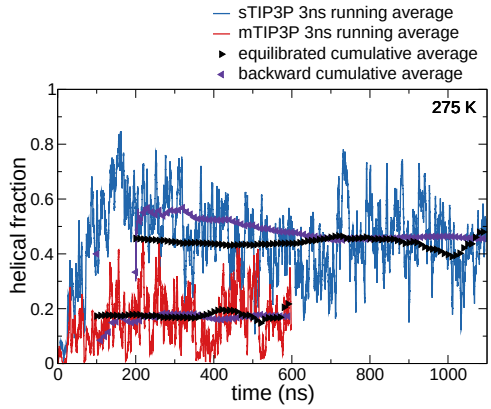

Figure 3.1: *Convergence of the helical fraction of the AQ peptide at 275 K. The running average, for the sTIP3P (blue) and for the mTIP3P (red) water model, uses a 3 ns window and starts at 0 ns, while the cumulative average (black) and backward cumulative average (purple) ignore the equilibration data.*

lies much closer to the experimental value at 300 K than mTIP3P, for both 3K(I) and GB1. The difference in the free energy of unfolding of 3K(I) between the two water models is about 4 kJ/mol at 275 K (see Figure 3.3).

The melting curves of AQ using sTIP3P or mTIP3P, shown in Figure 3.2b, lie on opposite sides of the experimental curve at lower temperatures, with deviations of 0.13 and −0.07 at 300 K. Figure 3.2b also shows the melting curve from a 50 ns run (after subtracting 100 ns equilibration time) with CHARMM36 and sTIP3P, produced by Best et al.[8] using a 2 ps exchange frequency. The helical fraction at 300 K from this run corresponds well with the helical fraction from the experiment. However, even for an equilibrated system of replicas, a 50 ns window might not be sufficient to determine an accurate average helical fraction. This can also be seen from the ruggedness of the Best et al.[8] melting curve, indicating that not all replicas have reached their equilibrium ensemble. In our simulations, using an even higher exchange frequency, an average helical fraction anywhere between 0.3 and 0.6 could be obtained when using a 50 ns window at distinct points after the equilibration (Figure 3.1). This illustrates the need for a longer time window to obtain an accurate average. The blue crosses in Figure 3.2a show that switching off the van der Waals potential between 10 and 12 Å yields results similar to the plain cut-off at 9 Å that was used otherwise.

3.3.2 Characteristics of the unfolded state

The parametrization of the CHARMM36 force field[10] was partly intended to rebalance the equilibrium between helical and extended conformations. In a search for the reason

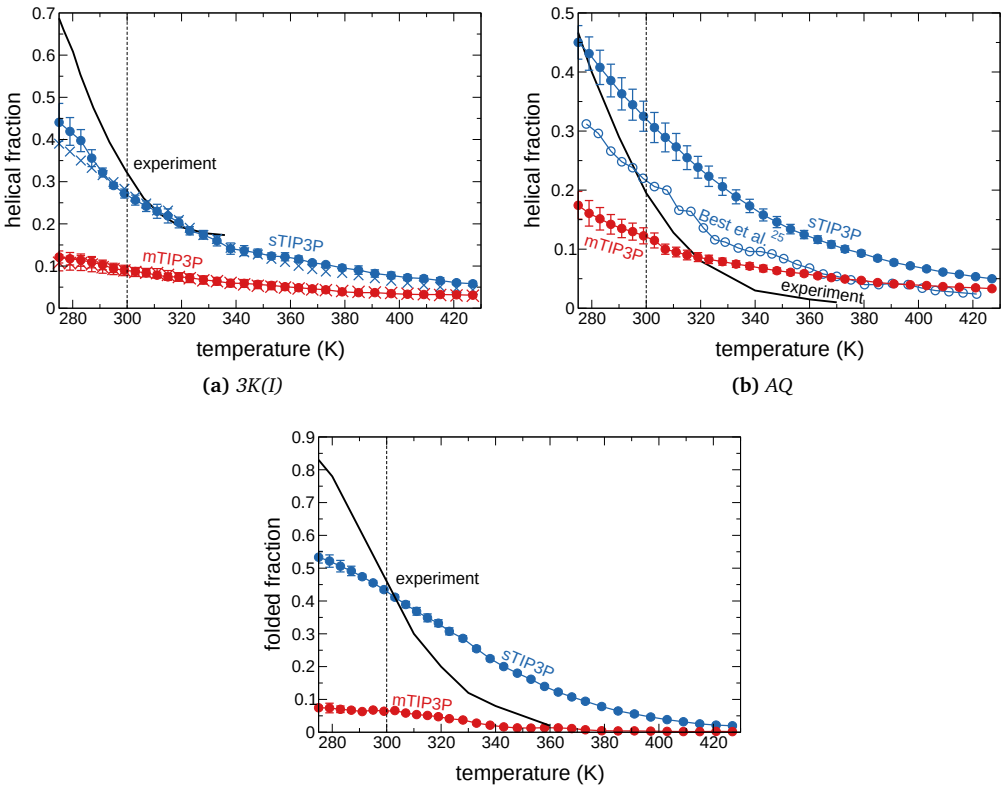

(a) *3K(I)* **(b)** *AQ*

(c) *GB1*

Figure 3.2: *Melting curves for the three tested peptides using the CHARMM36 force field combined with the sTIP3P (blue) and mTIP3P (red) water models. The crosses in (a) show the results using a van der Waals potential that is switched off between 10 and 12 Å interaction distance, instead of the 9 Å cutoff. The open circles in (b) show the result obtained with CHARMM36 and sTIP3P by Best et al.*[8] *The vertical dashed line at* 300 K *is drawn as a guide to the eye. Experimental results (black) from circular dichroism of 3K(I)*[26] *(a), NMR chemical shifts of AQ*[35] *(b), and tryptophan fluorescence of GB1*[29] *(c).*

underlying the differences seen above, we explore the effect of each of the water models on this balance. This effect is largest in the unfolded conformations, so we investigated these for the 3K(I) and GB1 peptides. The results for AQ (not shown) are similar to those for 3K(I) presented here.

Consistent with the results in Figure 3.2a, the unfolded 3K(I) peptide tends to more extended conformations in mTIP3P than in sTIP3P, as can be seen from the radius of gyration R_G of 3K(I) in Figure 3.4a (●, left axis). This suggests that unfolded molecules in mTIP3P tend to be more solvated, which is confirmed by a higher solvent accessible sur-

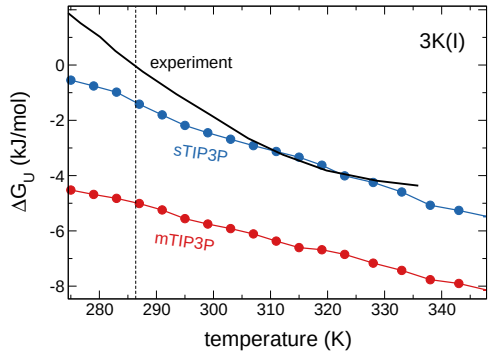

Figure 3.3: *Free energy of unfolding for the 3K(I) peptide using the CHARMM36 force field combined with the sTIP3P (blue) and mTIP3P (red) water models, calculated using* $\Delta G_U = -RT \ln[(1-x_H)/x_H]$ *with* x_H *the helical fraction. The vertical dashed line at the experimental melting point (*286 K*) is drawn as a guide to the eye. Experimental results (black) are extracted from circular dichroism of 3K(I).*[26]

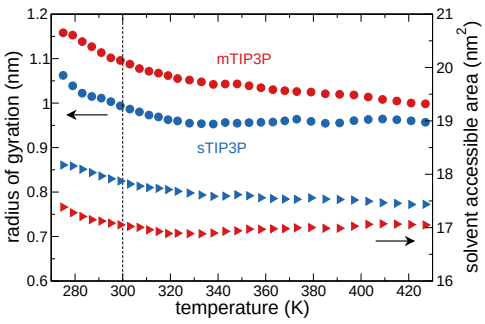

(a) *3K(I) is more extended in mTIP3P.*

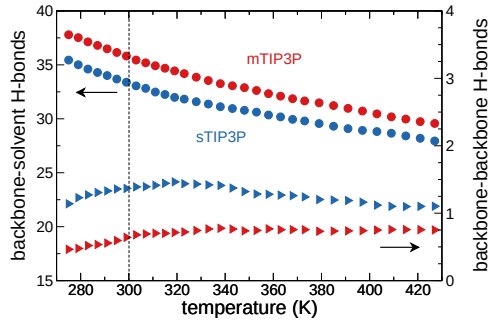

(b) *3K(I) has more backbone-backbone hydrogen bonds in sTIP3P.*

Figure 3.4: *Analysis of the unfolded conformations of 3K(I) for both water models (mTIP3P in red, sTIP3P in blue). (a) Radius of gyration (●, left axis) and solvent accessible surface area (►, right axis). (b) Hydrogen bond formation between backbone and solvent (●, left axis) and within the backbone (►, right axis). The vertical dashed line at* 300 K *is drawn as a guide to the eye. The symbols are larger than the errors.*

face area (SASA) of the unfolded peptide in this water model (Figure 3.4a, ►, right axis). The R_G of the unfolded state of 3K(I) can be compared to that of an almost identical peptide called AK16 (YGAAKAAAAKAAAAKA), measured to be 0.98 nm at room temperature in 4 M urea.[21] The R_G of 3K(I) in sTIP3P at room temperature is 0.99 nm, which lies significantly closer to the experimental value than the R_G of 1.10 nm in mTIP3P.

The higher solvation of the unfolded peptide in mTIP3P compared to sTIP3P can be

explained by stronger hydrogen bonding between the backbone and the solvent, as can be seen from the higher amount of backbone–solvent hydrogen bonds in Figure 3.4b (●, left axis). There is also less hydrogen bonding within the backbone of the peptide in mTIP3P (Figure 3.4b, ►, right axis) and consequently a less compact conformation. The R_G reduces with increasing temperature in both water models (Figure 3.4a). This corresponds to a slight increase in the number of backbone-backbone hydrogen bonds (Figure 3.4b), indicating collapse of the unfolded state by formation of secondary structure.

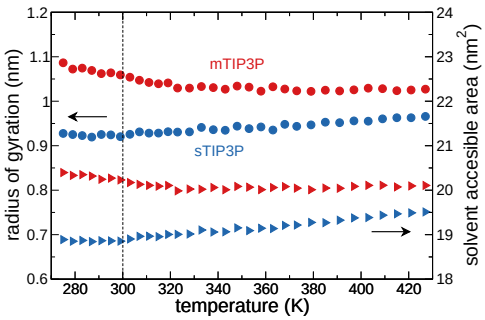

(a) *GB1 is more extended in mTIP3P.*

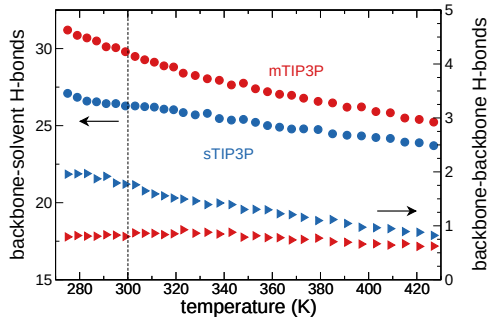

(b) *GB1 has more backbone-backbone hydrogen bonds in sTIP3P.*

Figure 3.5: *Analysis of the unfolded conformations of GB1 for both water models (mTIP3P in red, sTIP3P in blue). (a) Radius of gyration (●, left axis) and solvent accessible surface area (►, right axis). (b) Hydrogen bond formation between backbone and solvent (●, left axis) and within the backbone (►, right axis). The vertical dashed line at* 300 K *is drawn as a guide to the eye. The symbols are larger than the errors.*

The characteristics of the unfolded state of the GB1 hairpin look slightly different from the α-helical peptides, but the overall trend is the same. GB1 is also more extended and solvated in mTIP3P than in sTIP3P, as can be seen from the R_G and SASA in Figure 3.5a. Again, the number of backbone–solvent hydrogen bonds in Figure 3.5b (●, left axis) indicate that the higher solvation of the peptide in mTIP3P is due to stronger hydrogen bonding between the peptide and the solvent. Unlike the helical peptides, the β-hairpin does not show a collapse of the unfolded state in sTIP3P (Figure 3.5a). Inspection of the unfolded conformations of GB1 in sTIP3P shows that they are on average relatively compact because of a high amount of misfolded hairpins at low temperatures. This corresponds to the relatively high number of backbone-backbone hydrogen bonds, which gradually decrease with temperature (Figure 3.5b, ►, right axis).

3.4 Discussion

In the parametrization of the CHARMM36 force field, the backbone and side-chain dihedral angles were optimized in two separate steps. The simulations were done on several biomolecular systems that were solvated by either the sTIP3P or mTIP3P water model, depending on the molecular dynamics software used.[10] For instance, the backbone optimizations were performed using Ala_5 in mTIP3P and AQ in sTIP3P, with feedback from crystal simulations of folded proteins in mTIP3P. Side-chain optimizations were guided by simulations of unfolded GB1 and ubiquitin in urea and sTIP3P, as well as crystal simulations of proteins using mTIP3P. Validations have been carried out for several folded and unfolded proteins, using either sTIP3P or mTIP3P. Our results, however, show that there is a significant difference in the stability of helical and folded states between the two water models, which affects the applicability of the force field and water model to specific biomolecular systems.

There are other studies on peptides in the literature, in which the default water model has been replaced by an alternative one. A combination of Amber ff99SB with the TIP4P-Ew water model led to results that are consistent with those presented here.[31] The more extended unfolded conformations showed increased backbone–solvent hydrogen bonding which led to a significantly lower folded fraction of the Trp-cage miniprotein compared to that with the sTIP3P water model. The result of the sTIP3P simulation was recovered from the TIP4P-Ew simulation by reducing the backbone–solvent hydrogen bond strength. It was noted that enhancing the intramolecular peptide–peptide hydrogen bonds or strengthening the backbone dihedral potentials would lead to the same result. Such a rescaling stabilizes the folded state and increases the fraction of folded conformations at lower temperatures. Similarly, we expect that the helix–coil equilibrium for CHARMM36 in combination with mTIP3P could be restored by rescaling the hydrogen bond strength or readjusting the backbone dihedral potentials.

Another example of using an existing force field with a different water model is the optimization of Amber ff03w in combination with the TIP4P/2005 water model.[6] For this force field, the dihedral potentials of Amber ff03* were optimized against scalar couplings measured for Ala_5 and AQ. The resulting melting curve showed a higher helical fraction and increased cooperativity of folding using ff03w with TIP4P/2005, while the peptide was overall more extended than in ff03* with sTIP3P. Further analysis showed that the difference is related to a more favourable enthalpy of solvation in TIP4P/2005. In our simulations with CHARMM36, the peptides are more solvated in mTIP3P than in sTIP3P. In analogy to the results with Amber ff03w, we hypothesize that rebalancing the dihedral potentials of CHARMM36 for peptides solvated in mTIP3P could increase the amount of helical fraction and improve the cooperativity of helix formation with respect to our results in sTIP3P.

Further work on the Amber ff03w force field, resulting in the Amber ff03ws force field,

involved scaling of the Lennard-Jones interactions between atoms of the solute and oxygen atoms of the water molecules.[9] This scaling induced the intended reduction of protein–protein affinity, but also reduced the helical propensity of AQ in comparison with ff03w. This illustrates that increasing protein–solvent interactions involving the solvent oxygen atom can lead to a destabilization of the folded state, similar to the effect of the added interactions on solvent hydrogen atoms shown here in mTIP3P.

A recent comparison of force fields on the intrinsically disordered RS (24 residues) and FG-nucleoporin (16 and 50 residues) peptides has also shown that the combination of CHARMM36 with mTIP3P results in a more expanded peptide, with an R_G of the RS peptide that is about 1 Å larger than in sTIP3P.[34] This agrees with the difference in R_G that we found between the two water models for the three tested peptides of similar length. They have also found a high population (about 40%) of residues in a left-handed α-helical (α_L) conformation for the RS peptide in both water models. In the subsequently tested A_3 and AQ peptides, α_L was shown to be only 7%. This is consistent with our results, in which $\alpha_L \sim 5-7$ % (data not shown). Apparently, the secondary structure of intrinsically disordered peptides is not well-represented in CHARMM36 with either mTIP3P or sTIP3P, while peptides with more preference for a certain secondary structure are best represented when combined with sTIP3P.

The differences between the sTIP3P and mTIP3P water models are not substantial for simulations of proteins in their native, folded state. Backbone and side-chain NMR data have been compared with data from simulations in sTIP3P[10] and in mTIP3P,[10,18] both showing good correlation with experimental data. In the latter publication, utilization of mTIP3P was not declared specifically but confirmed to us by the authors (private communications). The water models also show negligible differences in the RMSD of folded proteins when combined with CHARMM27, the previous version of the force field.[11] Additionally, a force field comparison on folded proteins[27] reports little difference between the balanced and unbalanced (previous) versions of two Amber force fields. The native state of a folded protein in solution sits in a global free energy minimum that is apparently not affected much by the differences in solvation energy between the two water models. From this, we conclude that proteins with a low surface to volume ratio, which are consequently not highly solvated, can accurately be simulated using either of the water models. However, proteins with a high surface to volume ratio are expected to be influenced significantly by the water model.

For all molecular dynamics force fields, the parametrization conditions and settings are as much a part of the force field as the interaction potentials themselves. It is well-known that the water model is also an integral part of the parametrization.[23,24] Although the differences between the sTIP3P and mTIP3P water models are small in terms of bulk properties[11,25] and simulations of folded proteins, we have shown that they have a significant effect on the folding of small dynamic peptides. For these systems, CHARMM36 should best be used with sTIP3P, the water model it was parametrized with. Although there is

little difference between the two water models for simulations of folded proteins, we still recommend using sTIP3P because it reduces computational cost.

The CHARMM36 force field for proteins is often used for simulations including nucleic acids[14] or lipids.[20] The parameter set for nucleic acids has been optimized using sTIP3P, so combinations of proteins and nucleic acids can be readily simulated in sTIP3P water. For lipids, however, CHARMM36 was parametrized in combination with the mTIP3P water model. Using sTIP3P for a DPPC bilayer results in a significant underestimation of the area per lipid, with the bilayer transitioning into a tilted gel phase. This artifact occurs in particular when using the GROMACS switching function for the Lennard-Jones potential, which switches off the potential energies instead of the forces.[33] Hence, a combination of lipids with small dynamic peptides or natively unfolded proteins results in a conflict between the preferred water models and therefore requires reparametrization or rebalancing of one of the parameter sets to make them compatible with the water model used.

3.5 Conclusion

Comparison of the sTIP3P and mTIP3P water models using REMD on small dynamic peptides simulated with the CHARMM36 force field shows a better agreement with experimental melting curves if sTIP3P is used. The use of mTIP3P results in a more solvated and extended unfolded state, which in turn leads to a lower fraction of folded conformations. This appears to be due to a higher solvation energy of the peptide in this water model, shifting the balance from folded states toward more extended states.

For simulations of less dynamical systems, such as folded proteins in their native state, CHARMM36 could still be used in combination with mTIP3P water. This also holds for simulations that include lipids or nucleic acids. However, also regarding computational efficiency, we recommend using CHARMM36 in conjunction with sTIP3P when simulating small peptides, folded proteins, and dynamic or intrinsically unfolded proteins. The combination of dynamic peptides or proteins with lipids, parametrized using mTIP3P, requires a reparametrization to make the water models compatible.

References

[1] Avbelj F, Luo P, Baldwin R. 2000. Energetics of the interaction between water and the helical peptide group and its role in determining helix propensities. *PNAS* 97:10786–10791

[2] Basconi JE, Shirts MR. 2013. Effects of temperature control algorithms on transport properties and kinetics in molecular dynamics simulations. *J. Chem. Theory Comput.* 9:2887–2899

[3] Beauchamp KA, Lin YS, Das R, Pande VS. 2012. Are protein force fields getting better? A systematic benchmark on 524 diverse NMR measurements. *J. Chem. Theory Comput.* 8:1409–1414

[4] Best RB, Buchete NV, Hummer G. 2008. Are current molecular dynamics force fields too helical? *Biophys. J.* 95:L7–L9

[5] Best RB, Hummer G. 2009. Optimized molecular dynamics force fields applied to the helix-coil transition of polypeptides. *J. Phys. Chem. B* 113:9004–9015

[6] Best RB, Mittal J. 2010. Protein simulations with an optimized water model: Cooperative helix formation and temperature-induced unfolded state collapse. *J. Phys. Chem. B* 114:14916–14923

[7] Best RB, Mittal J. 2011. Free-energy landscape of the GB1 hairpin in all-atom explicit solvent simulations with different force fields: Similarities and differences. *Proteins* 79:1318–1328

[8] Best RB, Mittal J, Feig M, MacKerell AD. 2012. Inclusion of many-body effects in the additive CHARMM protein CMAP potential results in enhanced cooperativity of α-helix and β-hairpin formation. *Biophys. J.* 103:1045–1051

[9] Best RB, Zheng W, Mittal J. 2014. Balanced protein-water interactions improve properties of disordered proteins and non-specific protein association. *J. Chem. Theory Comput.* 10:5113–5124

[10] Best RB, Zhu X, Shim J, Lopes PEM, Mittal J, et al. 2012. Optimization of the additive CHARMM all-atom protein force field targeting improved sampling of the backbone ϕ, ψ and side-chain χ_1 and χ_2 dihedral angles. *J. Chem. Theory Comput.* 8:3257–3273

[11] Bjelkmar P, Larsson P, Cuendet MA, Hess B, Lindahl E. 2010. Implementation of the CHARMM force field in GROMACS: Analysis of protein stability effects from correction maps, virtual interaction sites, and water models. *J. Chem. Theory Comput.* 6:459–466

[12] Cino EA, Choy WY, Karttunen M. 2012. Comparison of secondary structure formation using 10 different force fields in microsecond molecular dynamics simulations. *J. Chem. Theory Comput.* 8:2725–2740

[13] García A, Sanbonmatsu K. 2002. α-Helical stabilization by side chain shielding of backbone hydrogen bonds. *PNAS* 99:2782–2787

[14] Hart K, Foloppe N, Baker CM, Denning EJ, Nilsson L, MacKerell AD. 2012. Optimization of the CHARMM additive force field for DNA: improved treatment of the BI/BII conformational equilibrium. *J. Chem. Theory Comput.* 8:348–362

[15] Hess B. 2008. P-LINCS: A parallel linear constraint solver for molecular simulation. *J. Chem. Theory Comput.* 4:116–122

[16] Hess B, Kutzner C, van der Spoel D, Lindahl E. 2008. GROMACS 4: Algorithms for highly efficient, load-balanced, and scalable molecular simulation. *J. Chem. Theory Comput.* 4:435–447

[17] Hornak V, Abel R, Okur A, Strockbine B, Roitberg A, Simmerling C. 2006. Comparison of multiple Amber force fields and development of improved protein backbone parameters. *Proteins* 65:712–725

[18] Huang J, MacKerell AD. 2013. CHARMM36 all-atom additive protein force field: Validation based on comparison to NMR data. *J. Comput. Chem.* 34:2135–2145

[19] Jorgensen WL, Chandrasekhar J, Madura JD, Impey RW, Klein ML. 1983. Comparison of simple potential functions for simulating liquid water. *J. Chem. Phys.* 79:926–935

[20] Klauda JB, Venable RM, Freites JA, O'Connor JW, Tobias DJ, et al. 2010. Update of the CHARMM all-atom additive force field for lipids: Validation on six lipid types. *J. Phys. Chem. B* 114:7830–7843

[21] Kohn JE, Millett IS, Jacob J, Zagrovic B, Dillon TM, et al. 2004. Random-coil behavior and the dimensions of chemically unfolded proteins. *PNAS* 101:12491–12496

[22] Lindorff-Larsen K, Maragakis P, Piana S, Eastwood MP, Dror RO, Shaw DE. 2012. Systematic validation of protein force fields against experimental data. *PLOS ONE* 7:e32131

[23] MacKerell AD, Bashford D, Bellott M, Dunbrack RL, Evanseck JD, et al. 1998. All-atom empirical potential for molecular modeling and dynamics studies of proteins. *J. Phys. Chem. B* 102:3586–3616

[24] Mackerell AD, Wiorkiewiczkuczera J, Karplus M. 1995. An all-atom empirical energy function for the simulation of nucleic-acids. *J. Am. Chem. Soc.* 117:11946–11975

[25] Mark P, Nilsson L. 2001. Structure and dynamics of the TIP3P, SPC, and SPC/E water models at 298 K. *J. Phys. Chem. A* 105:9954–9960

[26] Marqusee S, Robbins VH, Baldwin RL. 1989. Unusually stable helix formation in short alanine-based peptides. *PNAS* 86:5286–5290

[27] Martín-García F, Papaleo E, Gomez-Puertas P, Boomsma W, Lindorff-Larsen K. 2015. Comparing molecular dynamics force fields in the essential subspace. *PLOS ONE* 10:e0121114

[28] Miyamoto S, Kollman PA. 1992. Settle - An analytical version of the SHAKE and RATTLE algorithm for rigid water models. *J. Comput. Chem.* 13:952–962

[29] Muñoz V, Thompson PA, Hofrichter J, Eaton WA. 1997. Folding dynamics and mechanism of β-hairpin formation. *Nature* 390:196–199

[30] Neria E, Fischer S, Karplus M. 1996. Simulation of activation free energies in molecular systems. *J. Chem. Phys.* 105:1902–1921

[31] Paschek D, Day R, García AE. 2011. Influence of water-protein hydrogen bonding on the stability of Trp-cage miniprotein. A comparison between the TIP3P and TIP4P-Ew water models. *Phys. Chem. Chem. Phys.* 13:19840–19847

[32] Piana S, Klepeis JL, Shaw DE. 2014. Assessing the accuracy of physical models used in protein-folding simulations: Quantitative evidence from long molecular dynamics simulations. *Curr. Opin. Struct. Biol.* 24:98–105

[33] Piggot TJ, Pineiro A, Khalid S. 2012. Molecular dynamics simulations of phosphatidylcholine membranes: A comparative force field study. *J. Chem. Theory Comput.* 8:4593–4609

[34] Rauscher S, Gapsys V, Gajda MJ, Zweckstetter M, de Groot BL, Grubmüller H. 2015. Structural ensembles of intrinsically disordered proteins depend strongly on force field: A comparison to experiment. *J. Chem. Theory Comput.*

[35] Shalongo W, Dugad L, Stellwagen E. 1994. Distribution of helicity within the model peptide acetyl(AAQAA)$_3$amide. *J. Am. Chem. Soc.* 116:8288–8293